Preliminary investigations toward multi-frame DVB-S based passive ISAR

Fabrizio Santi[a], Iole Pisciottano[a,b], Diego Cristallini[b], Debora Pastina[a]
[a] Sapienza University of Rome – DIET Dept., Via Eudossiana 18, 00184, Rome, Italy
[b] Fraunhofer Institute for High Frequency Physics and Radar Techniques FHR – PSR Dept., Fraunhofer Str. 20, 53343, Wachtberg, Germany

Abstract

This paper investigates the possibility to combine passive ISAR imaging of a maneuvering ship over different frames using digital video broadcasting-satellite (DVB-S) as illuminators of opportunity. First, the image point spread function (PSF) in the target fixed reference system is analytically derived, allowing to characterize the resolution properties in a domain independent on the particular frame. Then, a few preliminary experimental results are provided considering a turning ferry, showing that the combination of multiple frame images can increase the amount of information enhancing the ship classification capability.

1 Introduction

Over the last years, ship detection has been one of the most popular research topics in the field of passive radar systems for maritime surveillance applications, while the study and development of radar techniques for advanced tasks such as ship classification are relatively new research lines. Relevant information such as ship size and shape can be extracted from inverse synthetic aperture radar (ISAR) images. In the past, some works focused on the ship target imagery using DVB-T illuminators [1]. The main merit in using such sources stays in the relatively high-transmitted power, as well as their widespread availability. However, the limited bandwidth can strongly affect the applicability of ISAR approaches for target classification and, most importantly, the imagery capability is limited at ships navigating on the coastal environment, as the transmitters are based on land.

In contrast to terrestrial-based radar systems, space-based passive radars provide a unique potential of persistent monitoring of even remote areas. Suitable candidates are navigation and communication satellites. With specific regard to ship ISAR imaging, [2] and [3] focus on GNSS-based passive radars, proving the possibility to obtain meaningful images exploiting such sources. However, the limited power budget of navigation satellites restricts the applicability of this technology at short-range applications, whereas communication satellites such as Inmarsat and Iridium, despite their better power budget, are less appealing for imagery purposes due to their limited bandwidth [4].

The exploitation of the digital broadcasting-satellite signals (DVB-S) seems a promising option for passive ISAR imaging [5]. Even though lower than the DVB-T case, the power budget is sensibly better than GNSS and each DVB-S transponder transmits signals over a bandwidth of few tens of MHz, being 32 MHz the most typical value, and there is the chance to process the signals transmitted by multiple transponders, enhancing the range resolution. In addition, the central frequency is comprised between 10.7 GHz and 12.75 GHz, potentially giving rise to high cross range resolution. Inspired by these benefits, recently some investigations have been conducted on ships ISAR imaging using a DVB-S-based passive radars [6-8].

In this work, we explore the possibility of combining multiple images acquired over different intervals (frames) to enhance the quality of the ISAR products. As the imaged target is moving, it is expected that different target scatterers can be visible to the radar over the different frames. Therefore, an image composed by the set of dominant scattering centers observed in the multiple frames can bring to a more reliable classification procedure [9].

In [7,8], the ship reflectivity is mapped into a target fixed reference system by means of back projection. Noticeably, this reference system is suitable for the combination of images acquired over different frames, where the variations of the effective rotation vector as well as the bistatic geometry modify the image projection plane (IPP), making ineffective the direct image combination in the more common range and Doppler plane. In order to provide a tool to characterize the spatial resolution properties of the images in this domain, we first derive the image point spread function (PSF) as a function of the ship axes (length, width and height). It is shown that under maneuvering motion, the shape of the PSF may considerably vary, giving rise to the possibility to select the more appropriate frame to retrieve specific characteristics of the target and/or to form a multi-frame image with enhanced resolution. The preliminary experimental results obtained by using a turning ferry as target of opportunity show that the multi-frame imagery could enhance the target information space, increasing the classification capability of the system.

The outline of this paper is as follows. Section II details the operative conditions and provides the derivation of the PSF. Experimental results are presented and discussed in Section III, while Section IV draws some conclusions.

2 DVB-S based passive ISAR

2.1 System geometry and signal model

The operative conditions are given by a DVB-S satellite as transmitter of opportunity (Tx) and a ground-based receiver (Rx) observing a ship target (TgT). As usually in

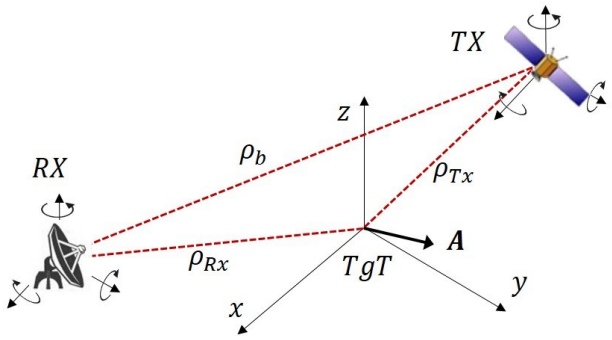

Figure 1 System geometry

passive radar, the receiver is equipped with two channels, one for reference (i.e., collecting the direct signal) and the other for surveillance. The target is modelled as a rigid body in the far field and we assume any relative translation between Rx/Tx and target fulcrum negligible (or already compensated) during the coherent processing interval (CPI). Therefore, the Rx-to-TgT, the Tx-to-TgT as well as the Tx-to-Rx (i.e., the baseline) distances, denoted respectively as ρ_{Rx}, ρ_{Tx} and ρ_b, are constant quantities. The target is assumed undergoing rotational motions, described by the vector $\boldsymbol{\omega} = [\omega_x, \omega_y, \omega_z]^T$, whose components account for the roll, pitch and yaw motions, respectively, and where the positive sign denotes a clockwise rotation.

The geometry of the system is depicted in **Figure 1**. The (0,X,Y,Z) is the target fixed reference system, where 0 denotes the ship fulcrum and X, Y and Z denote the directions of the longitudinal, lateral and vertical axes of the ship.

Let $\mathrm{P} = \{\mathrm{Rx}, \mathrm{Tx}\}$. At the reference time instant $u = 0$, P lies on the direction defined by the vector

$$\boldsymbol{\Phi}_\mathrm{P} = [\cos\theta_\mathrm{P} \cos\psi_\mathrm{P}, \sin\theta_\mathrm{P} \cos\psi_\mathrm{P}, \sin\psi_\mathrm{P}]^T \qquad (1)$$

where θ_P and ψ_P are the aspect angle (counterclock-wise from X-axis) and the elevation angle, respectively. In the considered reference system, P rotates around the target with motion described by the rotation matrixes M_x, M_y and M_z accounting for the roll, pitch and yaw (counter-clockwise rotations). Therefore, its instantaneous positions are given by

$$\mathbf{P}(u) = \rho_\mathrm{P} M_z M_y M_x \boldsymbol{\Phi}_\mathrm{P} \qquad (2)$$

The received signal from a point scatterer $\boldsymbol{A} = [x, y, z]^T$ belonging to the target body can be written in the fast-time & slow-time (t, u) domain as

$$h_A(t,u) = s[t - \tau_A(u)]\, e^{-j2\pi f_{d_A}(u)t}\, e^{-j2\pi f_c \tau_A(u)} \qquad (3)$$

where $s(t)\exp\{j2\pi f_c t\}$ is the transmitted signal, $\tau_A(u)$ and $f_{d_A}(u)$ are the instantaneous time delay and Doppler frequency, and f_c is the carrier frequency.

2.2 Point Spread Function

The system PSF expressed in the target fixed reference system can be obtained from the generalized ambiguity function, which can be expressed in the fast frequency & slow-time (f, u) domain as [10]

$$\chi(\boldsymbol{A}) = \frac{\iint h_0(f,u) h_A^*(f,u)\, df\, du}{\sqrt{\iint |h_0(f,u)|^2\, df\, du}\sqrt{\iint |h_A(f,u)|^2\, df\, du}} = \\ = \int \left(G(f)\, \mathrm{e}^{j2\pi f \tau_d(u)} \times \int_{-\frac{T_f}{2}}^{\frac{T_f}{2}} \mathrm{e}^{j2\pi f_c \tau_d(u)} du \right) df \qquad (4)$$

where h_0 is the received signal from the target fulcrum, $\tau_d(u) = \tau_A(u) - \tau_0$ is the differential time delay between $\boldsymbol{A}$ and target fulcrum, T_f is the frame duration (CPI) and $G(f)$ is the normalized power spectrum of the transmitted signal.

Taking into account the limited size of the targets of interest, $\tau_d(u)$ can be approximated in Taylor series around the fulcrum position arresting the series at the first order. Moreover, assuming negligible (or otherwise compensated) range migrations within the CPI, the exponential term in the outer integral of (4) can be approximated by the delay at the image time. Carrying out the calculus and by setting $\boldsymbol{\Theta} = \boldsymbol{\Phi_{Rx}} + \boldsymbol{\Phi_{Tx}}$, we obtain

$$\tau_d^0 = -\frac{\boldsymbol{\Theta}^T \boldsymbol{A}}{c} \qquad (5)$$

c being the speed of light.

In the inner integral, the term τ_d in the argument of the $exp(\cdot)$ term can be approximated with a Taylor series around $u = 0$. Accounting for negligible (or otherwise compensated) Doppler migration within the CPI, the series can be arrested at the first order, i.e., $\tau_d(u) \approx \tau_d^0 + \dot{\tau}_d u$. From (2), $\dot{\tau}_d$ is obtained as

$$\dot{\tau}_d = -\frac{1}{c} \boldsymbol{\omega}^T \boldsymbol{g}\{\boldsymbol{\Theta}\} \qquad (6)$$

$\boldsymbol{g}$ being the operator transforming a [3×1] vector in an antisymmetric matrix.

With the above positions, neglecting the constant scale factors, (4) can be reduced as

$$\boldsymbol{\chi}(\boldsymbol{A}) = e^{-j\frac{2\pi}{\lambda}\boldsymbol{\Theta}^T \boldsymbol{A}} g\left(\frac{\boldsymbol{\Theta}^T \boldsymbol{A}}{c}\right) sinc\left[\frac{T}{\lambda} \boldsymbol{\omega}^T (\boldsymbol{\Theta} \wedge \boldsymbol{A})\right] \qquad (7)$$

$\wedge$ denoting the cross product, λ the wavelength and $g(\cdot)$ the time response of the DVB-S signal. As a generalized form of $g(\cdot)$ is not currently available [11], at this stage, it is modeled as a *sinc* function.

As case study, let us assume a target under maneuver characterized by $\boldsymbol{\omega} = [0.3\ 0.2\ 3]\ °/s$ (i.e., dominant yaw) and a signal bandwidth of 25 MHz. Without loss of generality, we assume such motion conditions stationary over an overall aperture time equal to 10 s. Let the overall dwell segmented in 20 frames each having duration 0.5 s. At the reference instant, Rx is located in [1,0,0] km, whereas Tx illuminates the target with $\psi_{Tx} = 33°$ and $\theta_{Tx} = 45°$ at a distance of 38000 km.

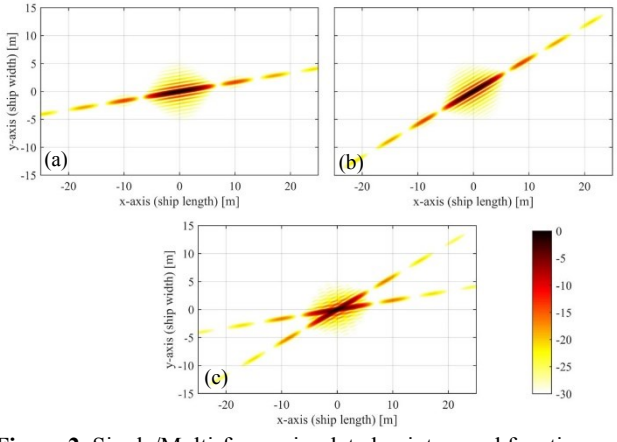

Figure 2 Single/Multi-frame simulated point spread functions – (a) frame 4, (b) frame 18, (c) frame 4 + frame 18

(a) (b)

Figure 3 Receiving system (a) and cooperative target (b)

Figure 2 (a) and (b) show the PSFs concerning the 2nd and 18th frames. As it is apparent, in the target fixed reference system, the system PSF has an elliptical shape, whose orientation varies with the relative Tx-TgT-Rx positions, here changing with the frame time due to the target maneuvers. Because of the different orientation of the PSF over the different frames, particular frames can be more appropriate to extract the ship length or the ship width. Moreover, depending on their relative positions, multiple scatterers that cannot be resolved in a particular frame could become distinguishable in another frame. Eventually, a multi-frame image with potentially higher resolution could be obtained by non-coherent summation [12], as shown in Figure 2 (c).

3 Experimental results

Experiments were conducted by means of the passive radar system SABBIA developed at Fraunhofer FHR. The passive radar is exploiting broadcast satellite DVB-S(2) signals emitted in Ku-band from geostationary satellites. SABBIA is based on two identical receiver front-ends, one for surveillance and the other for reference, each connected to a dish antenna as can be seen in **Figure 3** (a). More details of the SABBIA system can be found as well in [7].

The system was installed on the bank of the Rhine near Bonn, Germany. During the experiment, the satellite Astra 19.2° was exploited as illuminator of opportunity and a bistatic angle of about 36° was experienced. The signals transmitted by an individual transponder around the central frequency 11.362 GHz, over a nominal bandwidth of 32 MHz, have been acquired. The target of opportunity was the Königswinter ferry [Figure 3 (b)], having length 46.24 m and width 20 m. The target was equipped with an inertial measurement unit (IMU), providing information about the ferry position and motion. During the acquisition, the ferry underwent a full rotation, giving us the possibility to image it over a wide set of viewing angles.

The ISAR processing, comprising range compression, target detection, ship segment extraction, and known-motion back projection [7], has been applied to the different frames with $T_f \in [0.2 - 0.8]$s.

To experimentally obtain a single frame PSF and compare it with the theoretical result we selected an individual frame with duration 0.2 s where an isolated point-like scatterer is well visible. The focused image is shown in **Figure 4** (a), where a quite isolated bright return is easily recognized, while Figure 4 (b) shows the theoretical PSF (7). This has been obtained by using the IMU information to

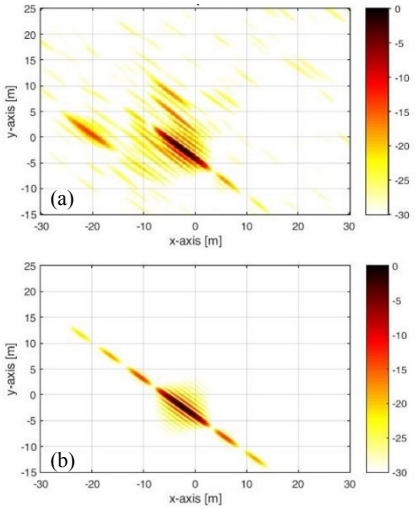

Figure 4 Experimental (a) and theoretical (b) PSF

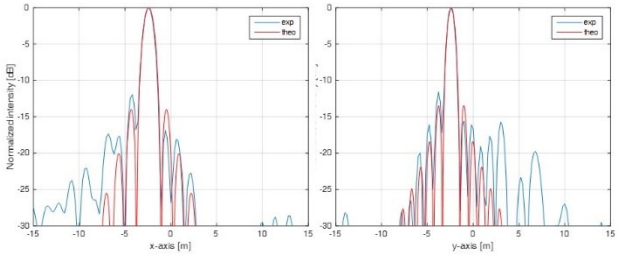

(a) (b)

Figure 5 Cuts along the X (a) and Y (b) axes. The blue curves correspond to the cuts over experimental PSF as in Figure 4(a); the red curves correspond to the cuts over theoretical PSF as in Figure 4(b)

Table I Acquisition parameters

Frame n.	T_f [s]	$\boldsymbol{\omega} = [\omega_x\ \omega_y\ \omega_z]$ [deg/s]	θ_{Rx}, ψ_{Rx} [deg]	θ_{Tx}, ψ_{Tx} [deg]
22	0.4	[-0.01 0.03 3.99]	172.2, 2.2	171.7, 33.0
23	0.4	[-0.01 -0.02 2.83]	-168.4, 2.5	-168.6, 33.3
27	0.8	[-0.01 -0.01 1.03]	-134.5, 2.8	-135.3, 33.6

define the vector $\boldsymbol{\omega}$, whereas as signal bandwidth a value equal to 25 MHz has been considered by evaluating the significant portion of the acquired spectrum. As it is apparent, experimental and theoretical results are in nice correspondence, as also confirmed by the comparison of the cuts along the X- and Y-axes (**Figure 5**). Particularly, it has to be pointed out that the same orientation of the simulated and theoretical PSF has been obtained.

Figure 6 shows three images of the ferry achieved in three different frames, whose parameters are reported inTble I. The black star markers superimposed to the images represent the corners of the ferry, whereas the blue diamond marker is the position of the IMU (target fulcrum). 0 dB denotes the noise background. As it is apparent, the images are composed by a number of elliptical spots of different size and orientation depending on the particular frame. (These show to be in nice correspondence with the theoretical PSFs.) Apart the different resolution properties of the images, it can be observed how different portions of the ferry gave rise to bright returns in the different images,

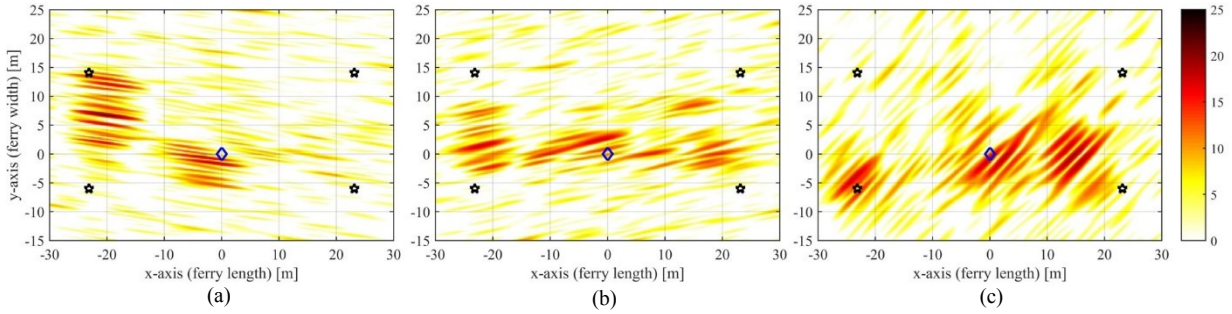

Figure 6 Experimental single frame images - (a) frame 22, (b) frame 23, (c) frame 27

consequently the different orientation of the target with respect to the receiver due to its maneuvering motion. Comparing the images with the receiver viewing angles in Table I, it could be observed that the brighter parts of the ferry are the ones directly facing the receiver line of sights. The different shadowing effects could be overcame via multi-frame imagery.

Figure 7 show few examples of multi-frame images. Figure 7 (a) shows the image obtained by non-coherent addition of frames 22 and 23, and Figure 7 (b) is the result of the combination of frames 22 and 27. As it is apparent, a more precise identification of the left edge is visible in the Figure 7 (a), and both the left and bottom segments can be recognized in Figure 7 (b), as a consequence of the wider variation of the radar perspective. In addition, it should be pointed out that a not excessive variation of the target orientation is experienced between frames 22 and 23 (~20°), so that bright returns are visible in the same regions. At the same time, the PSF are differently oriented, so that in the multi-frame image in Figure 7 (a) there is the chance to isolate more precisely individual scattering points.

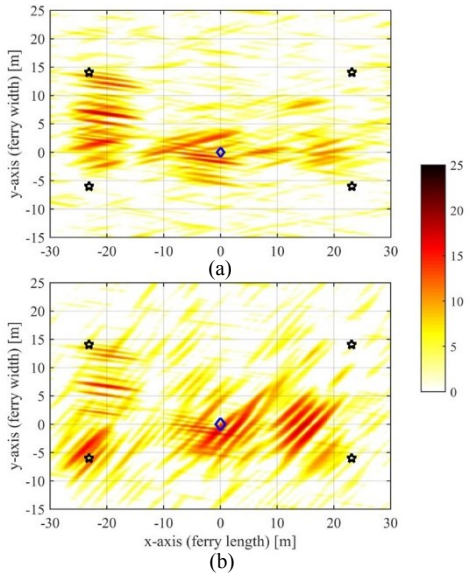

Figure 7 Experimental multi-frame images - (a) frame 22 + frame 23, (b) frame 22 + frame 27

4 Conclusions

In this paper, we presented a preliminary investigation about multi-frame ISAR imaging of ship targets exploiting DVB-S illuminators of opportunity.

As different frames can reveal different features of the ships, combining multiple frames can improve the diversity of visible scattering centers, providing a more comprehensive image for classification purposes. Moreover, as proved by the PSF evaluation, individual scatterers may give rise to differently oriented bright spots in the multiple frame, potentially enabling multi-frame imaging with enhanced resolution.

References

[1] D. Olivadese, E. Giusti, M. Martorella, *et al*., Passive ISAR with DVB-T signals, IEEE Trans. GRS, vol. 51 (8), pp. 4508-4517, Aug. 2013.

[2] D. Pastina, F. Santi, F. Pieralice, *et al*., Passive radar imaging of ship targets with GNSS signals of opportunity, IEEE Trans. GRS, *in press*.

[3] F. Santi, D. Pastina, M. Antoniou, M. Cherniakov, GNSS-based multistatic passive radar imaging of ship targets, IEEE RadarConf, 2020, pp. 601-606.

[4] A. G. Stove, M. S. Gashinova, S. Hristov, M. Cherniakov, Passive maritime surveillance using satellite communication signals, IEEE Trans. AES, vol. 53 (6), pp. 2987-2997, Dec. 2017.

[5] S. Brisken, M. Moscardelli, V. Seidel, C. Schwark, Passive radar imaging using DVB-S2, IEEE Radar Conf., 2017, pp. 552-556.

[6] T. V. Cao, R. Melino, H.-T. Tran, Using passive ISAR for imaging maritime targets, Int. Radar Symp., 2019, Ulm, Germany.

[7] I. Pisciottano, D. Cristallini, D. Pastina, Maritime target imaging via simultaneous DVB-T and DVB-S passive ISAR, IET RSN, vol. 13 (9), pp. 1479-1487, Sep. 2019.

[8] I. Pisciottano, F. Santi, D. Pastina, D. Cristallini, DVB-S based passive polarimetric ISAR – methods and experimental validation, IEEE Sensors Journal, *in press*.

[9] S. Brisken, J. G. Worms, Incoherent addition of ISAR images from spatially distributed receivers for classification purposes, Int. Radar Symp., 2010, Vilnius, Lithuania.

[10] T. Zeng, M. Cherniakov, T. Long, Generalized approach to resolution analysis in BSAR, IEEE Trans. AES, vol. 41 (2), pp. 461-474, Apr. 2005.

[11] Z. Sun, T. Wang, T. Jiang, *et al*., Analysis of the properties of DVB-S signal for passive radar applications, Int. Conf. on Wireless Comm. and Sign. Proc., Hangzhou, China, 2013.

[12] F. Santi, M. Antoniou, D. Pastina, Point spread function analysis for GNSS-based multistatic SAR, IEEE GRSL, vol. 12 (2), pp. 304-308, Feb. 2015.